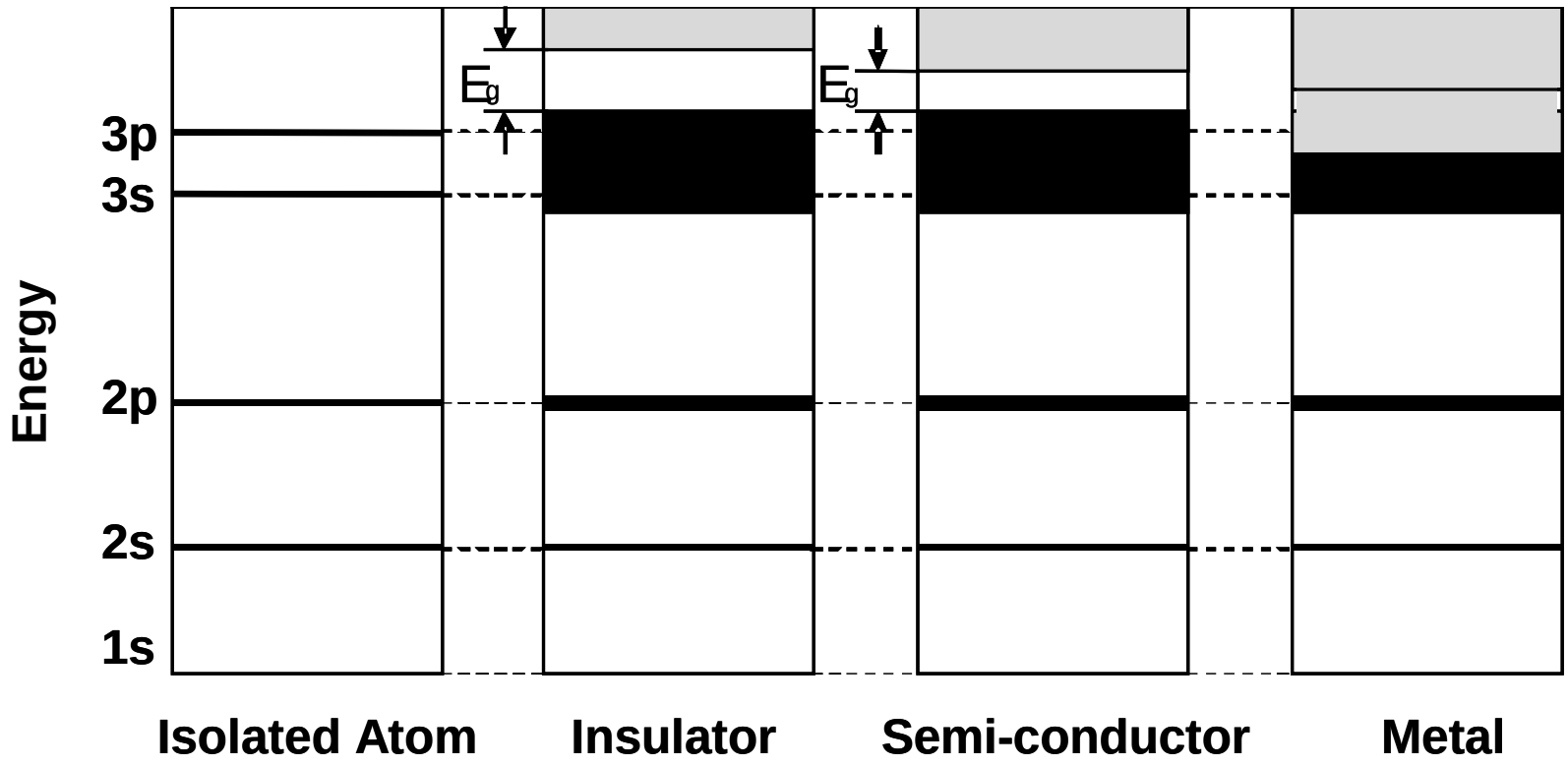

Figure 26.1. Various energy levels of isolated atom, insulator, semi-conductor and metal. The grey shaded region represents the lowest unoccupied energy band at ground state known as conduction band. The dark region is the valence band that is fully filled with valence electrons. These conduction and valance bands are separated by a bandgap denoted by E_g.

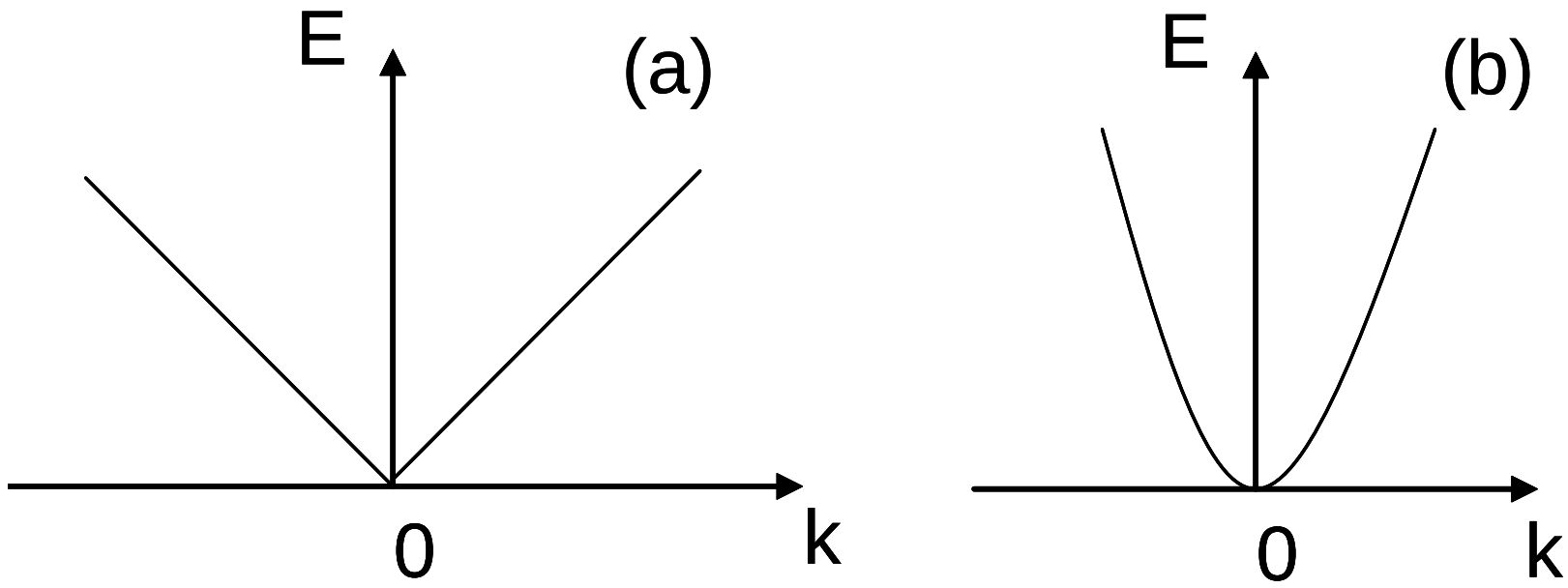

Figure 26.2 Dependence of energy on wave-vector in free space for (a) photons; (b) electrons.

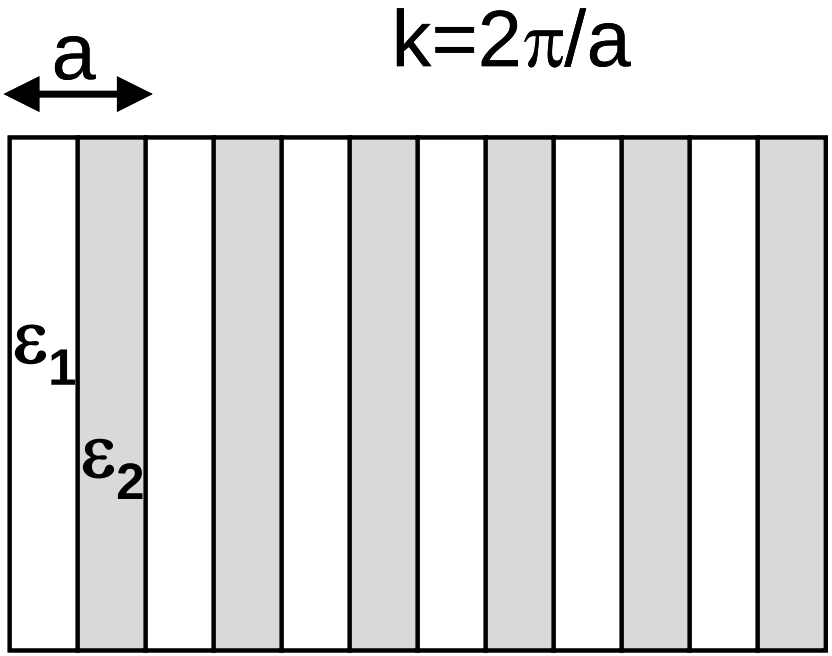

Figure 26.3 Illustration of materials exhibiting one-dimensional periodic variation of dielectric constant.

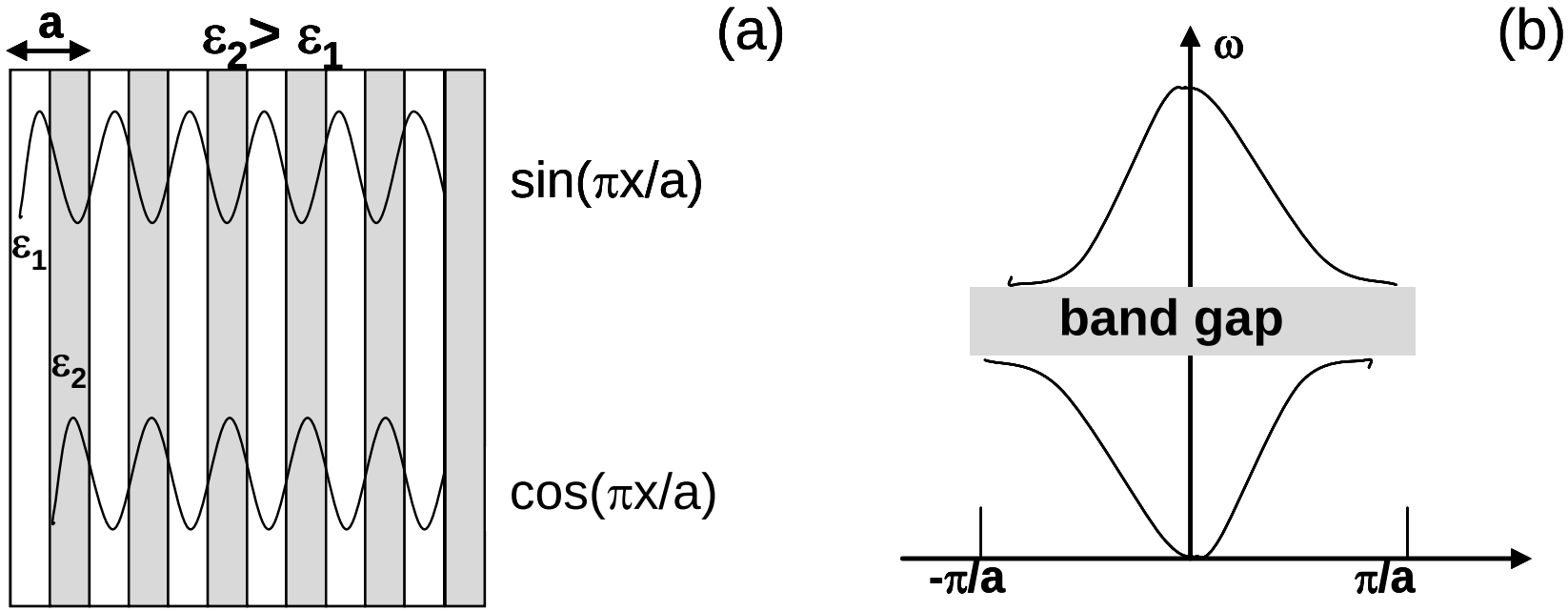

Figure 26.4 (a) Schematic representation of a plane wave splitting into two standing waves. (b) Illustration of a photonic gap in between the high frequency band and low frequency band.

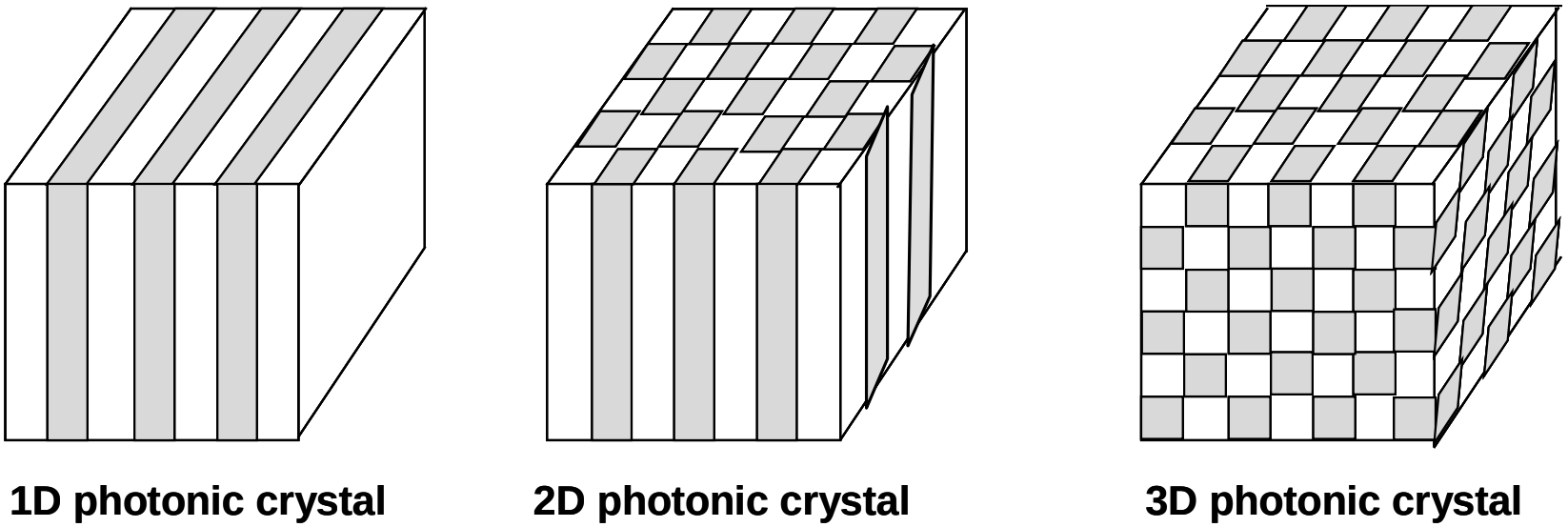

Figure 26.5 Schematic representations of 1D, 2D, and 3D photonic crystals having 1, 2 and 3 dimensional periodicity, respectively.

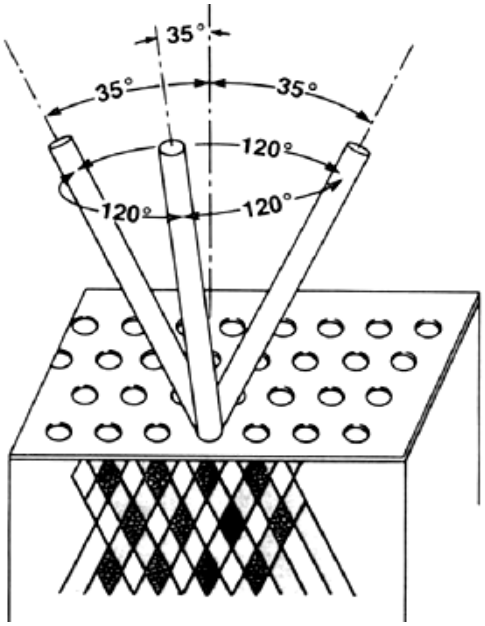

(a)

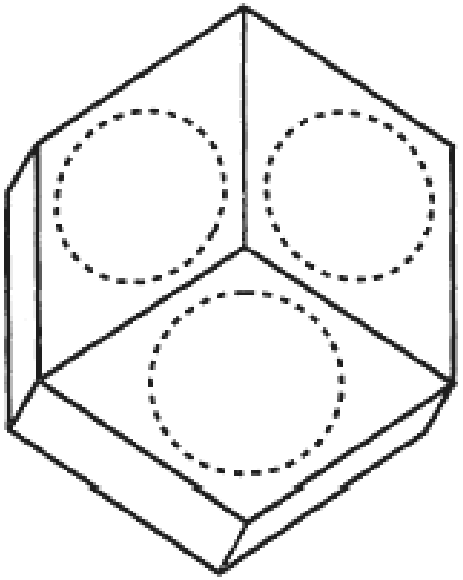

(b)

Figure 26.6 Schematic representation of (a) mechanical drilling method to construct an fcc crystal structure illustrated in (b). (Reproduced with permission from American Physics Society and authors; Reference 18).

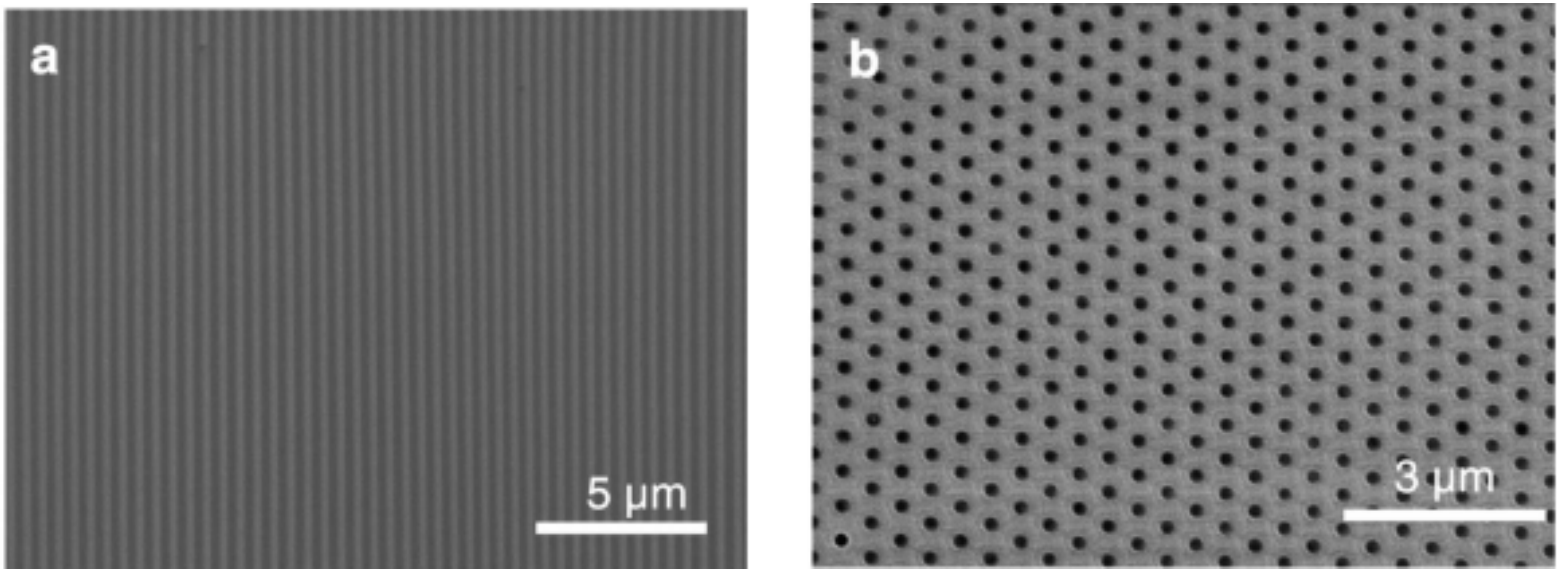

Figure 26.7 SEM images of porous alumina structure fabricated by the anodization of pre-patterned aluminum: a) side view; b) top view (Reproduced with permission from American Institute of Physics and authors; Reference 19).

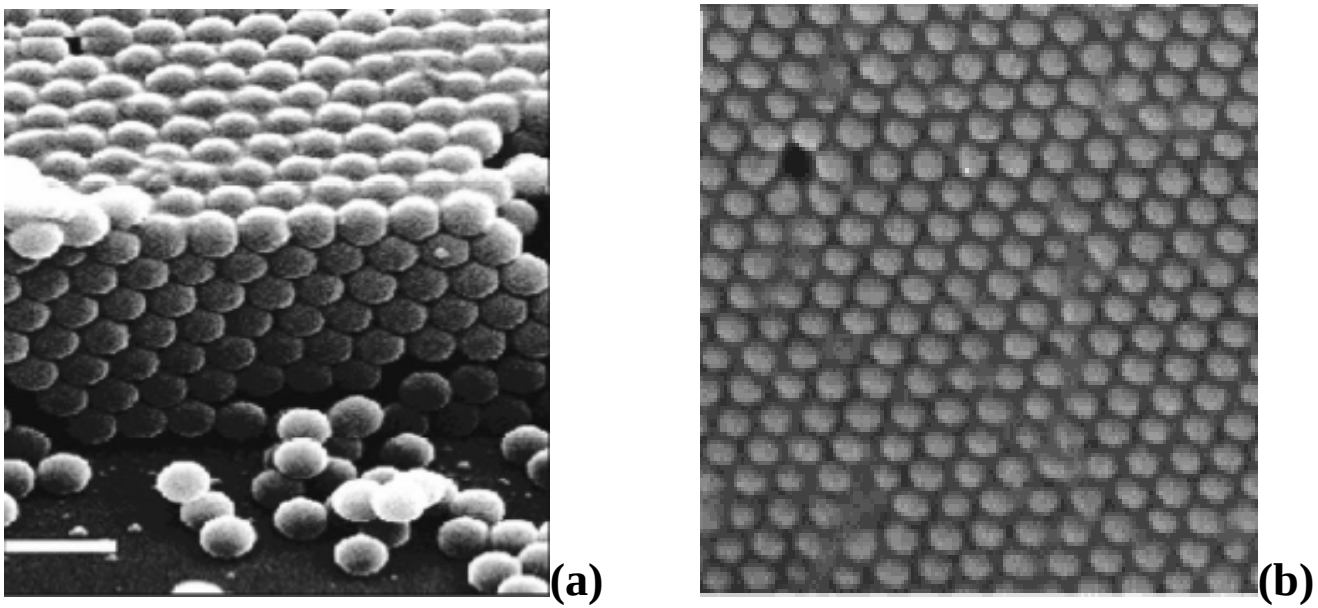

Figure 26.8 3D photonic crystals formed by self-assembly of (a) silica colloids (Reproduced with permission from Material Research Society and author in reference 23) and (b) polystyrene spheroids (from reference 30). The scale bar in (a) is 1 μm. (Reproduced with permission from American Chemical Society and authors; Reference 30).

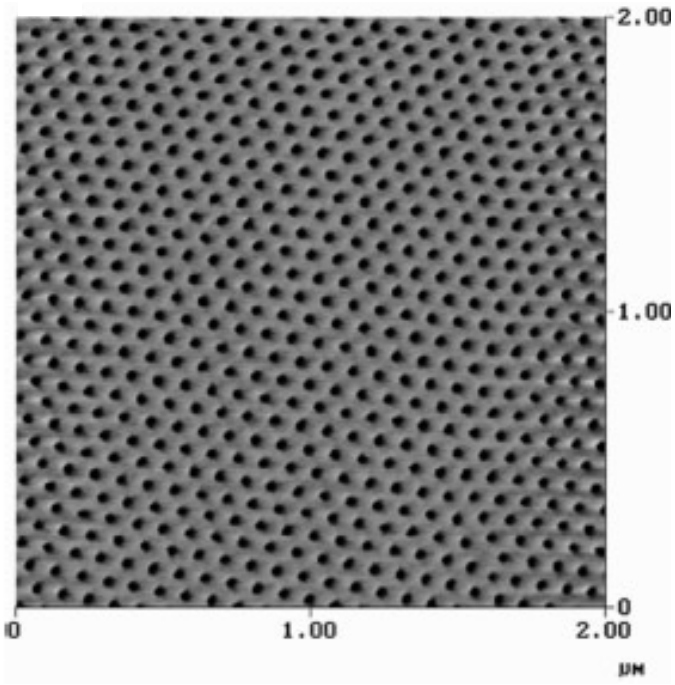

Figure 26.9 AFM image of the highly ordered cylindrical array structures grown from the solvent evaporation of self-assembled PS-b-PEO block copolymer film (Reproduced with permission from John Wiley & Sons and authors; Reference 32).

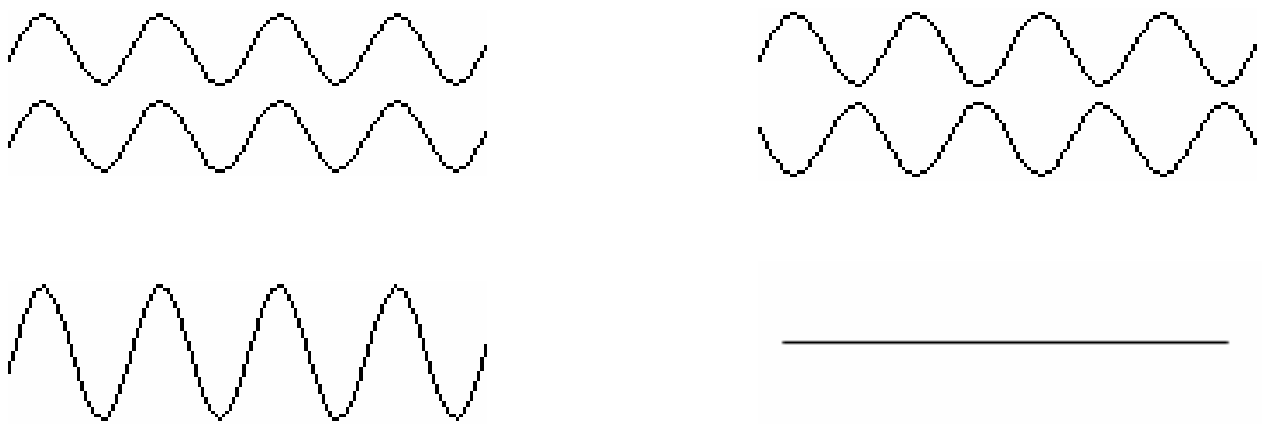

a) Constructive Interference **b) Destructive Interference**

Figure 26.10 Conceptual illustration of constructive and destructive interference in two-wave interference.

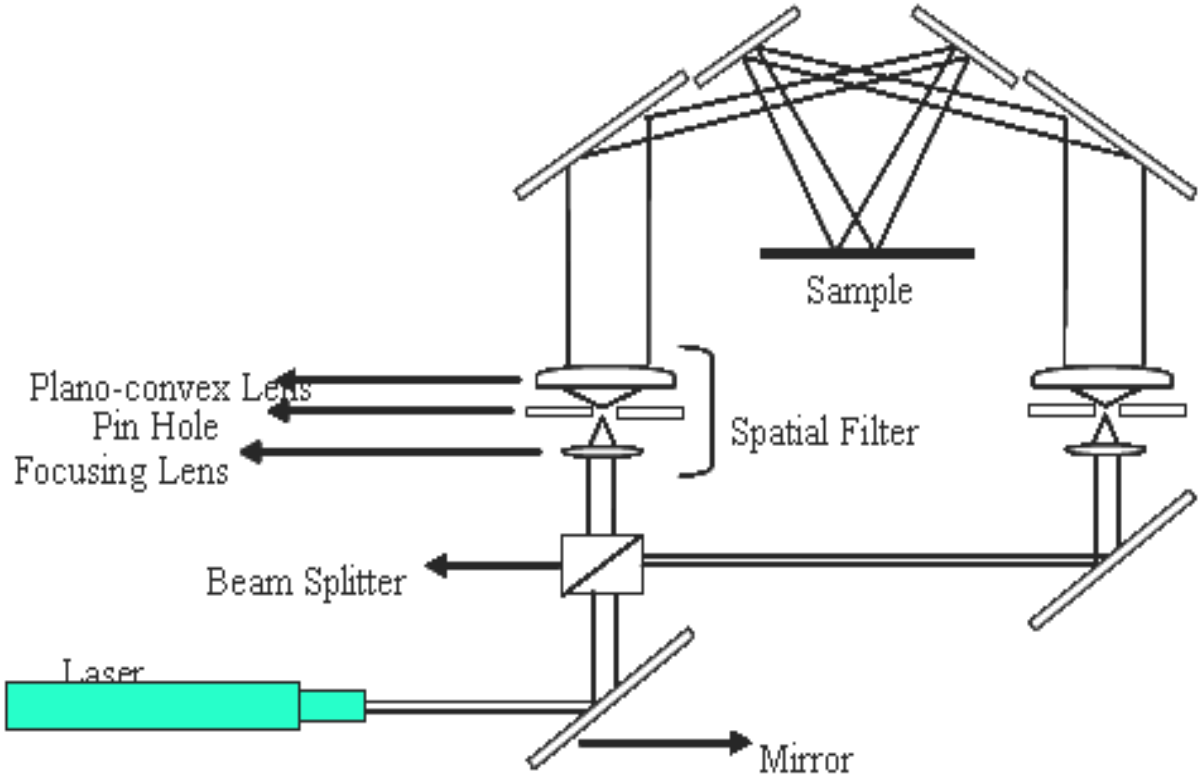

Figure 26.11 Schematic representation of the optical set-up based on two-wave interference concept.

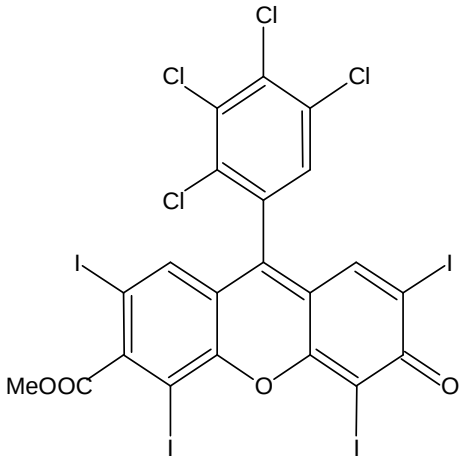

RBAX– Rose Bengal derivative
(Spectra Group Inc.)

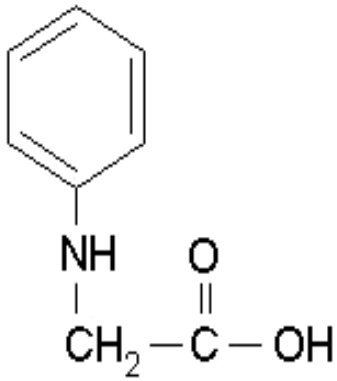

N-Phenyl Glycine
(co-initiator)

Figure 26.12 Chemical structures of typical initiator, co-initiator, solubilizing agent, and surfactant in an initiating system of photo-reaction.

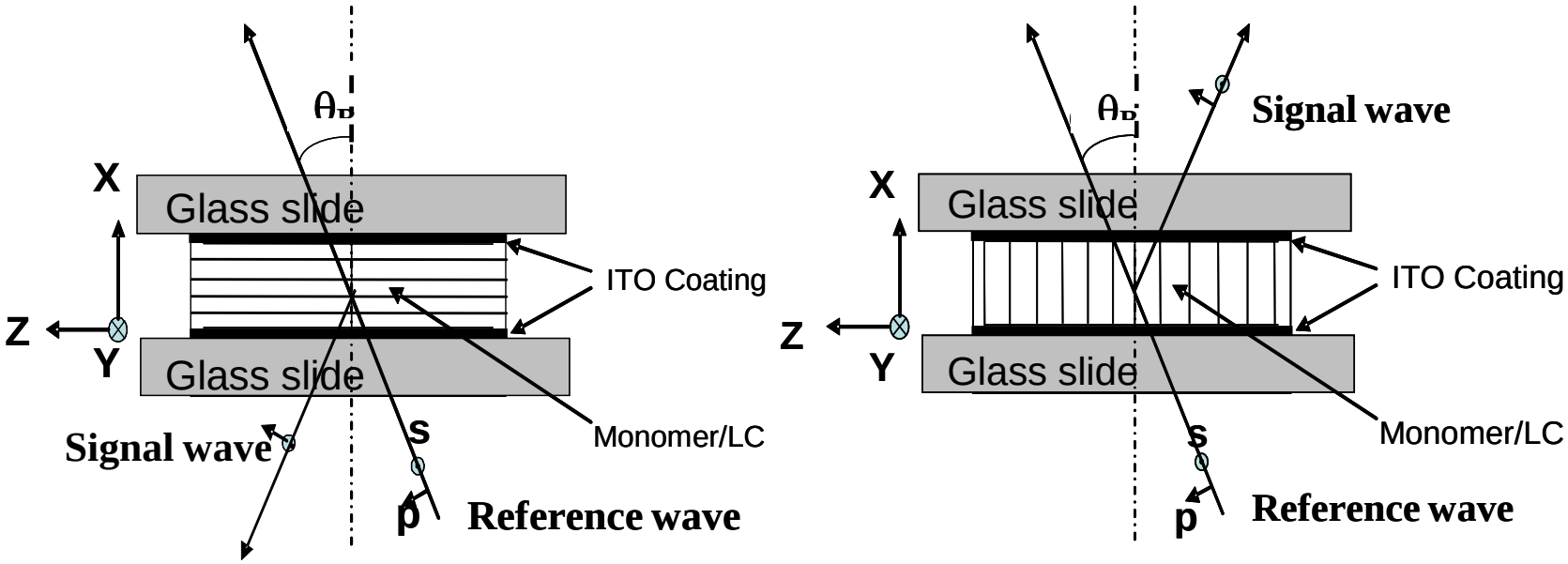

Figure 26.13 Schematic illustrations of reflection grating (left) and transmission grating (right).

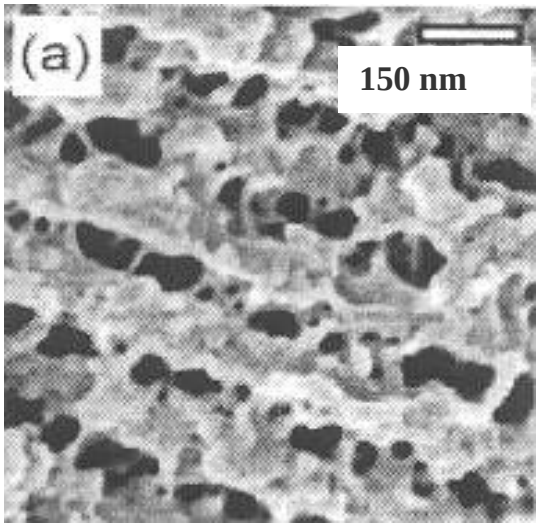

Experiment

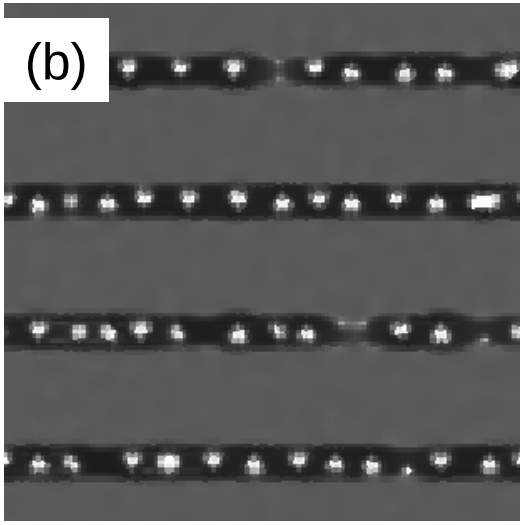

Simulation

Figure 26.14 Comparison of SEM morphology of pentacrylate based H-PDLC after extraction of LC (left) with the simulated one (right) showing the LC domains in stratified layers.

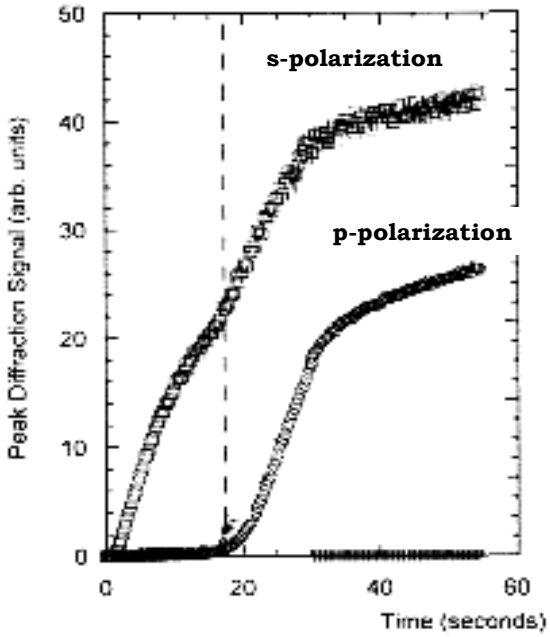

Experiment

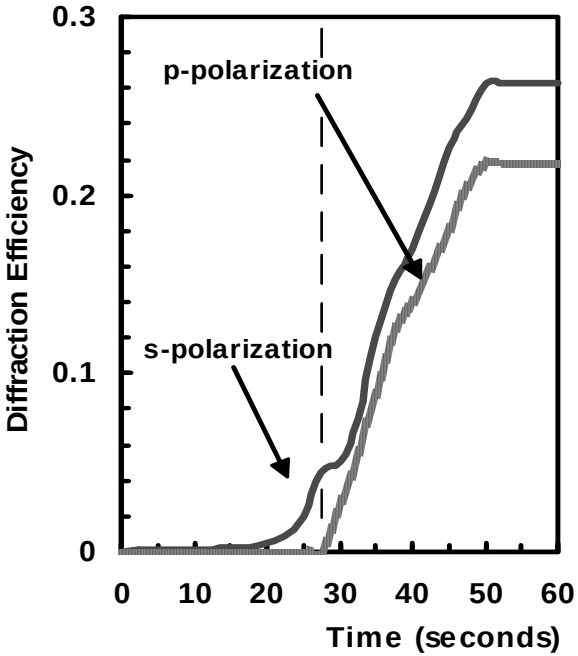

Simulation

Figure 26.15 Comparison of diffraction efficiency evolution from in-situ experimental measurement (left) with the simulated result (right).

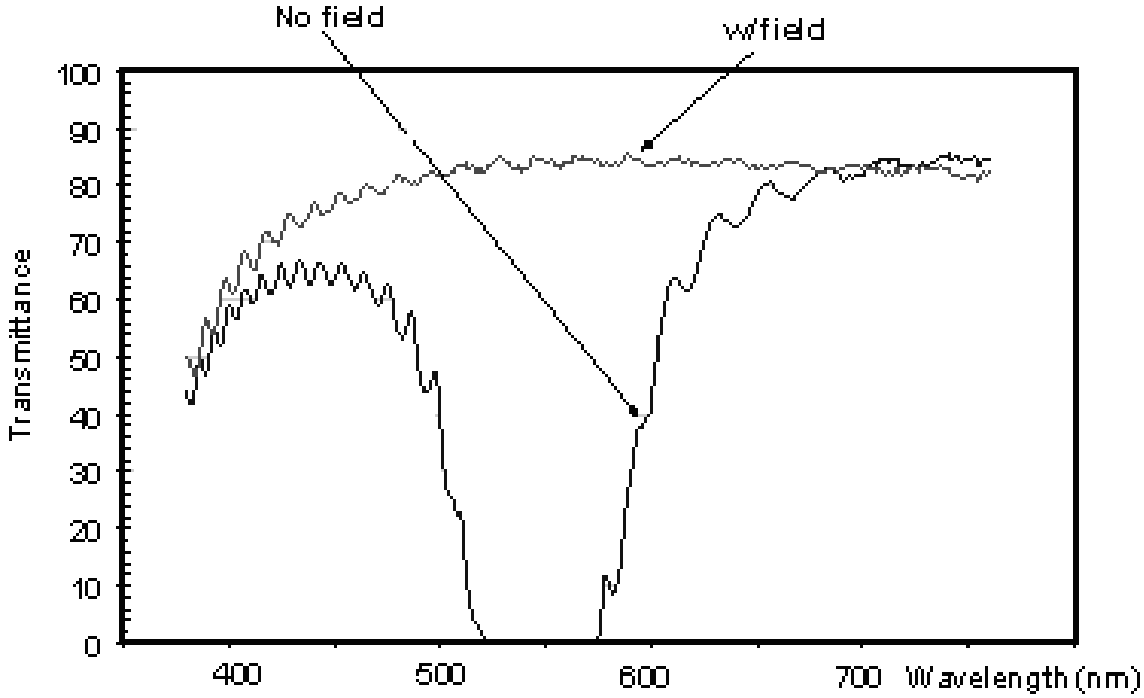

Figure 26.16 Illustration of the notch filter fabricated from PBG material with control of external electric field to switch it on and off (Courtesy of T. J. Bunning).

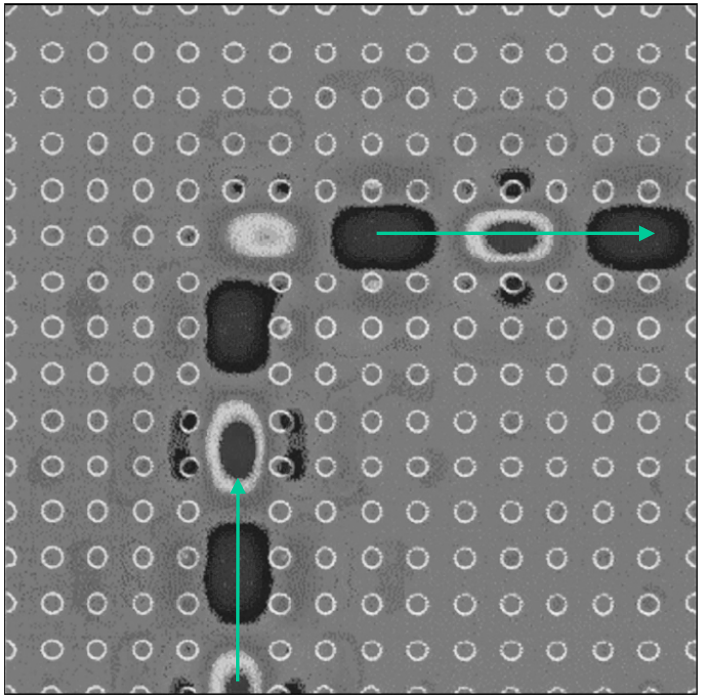

Figure 26.17 Theoretical calculations based on a defect pathway allow a 90° sharp bending of light propagation (Reproduced with permission from Material Research Society and authors; Reference 22).

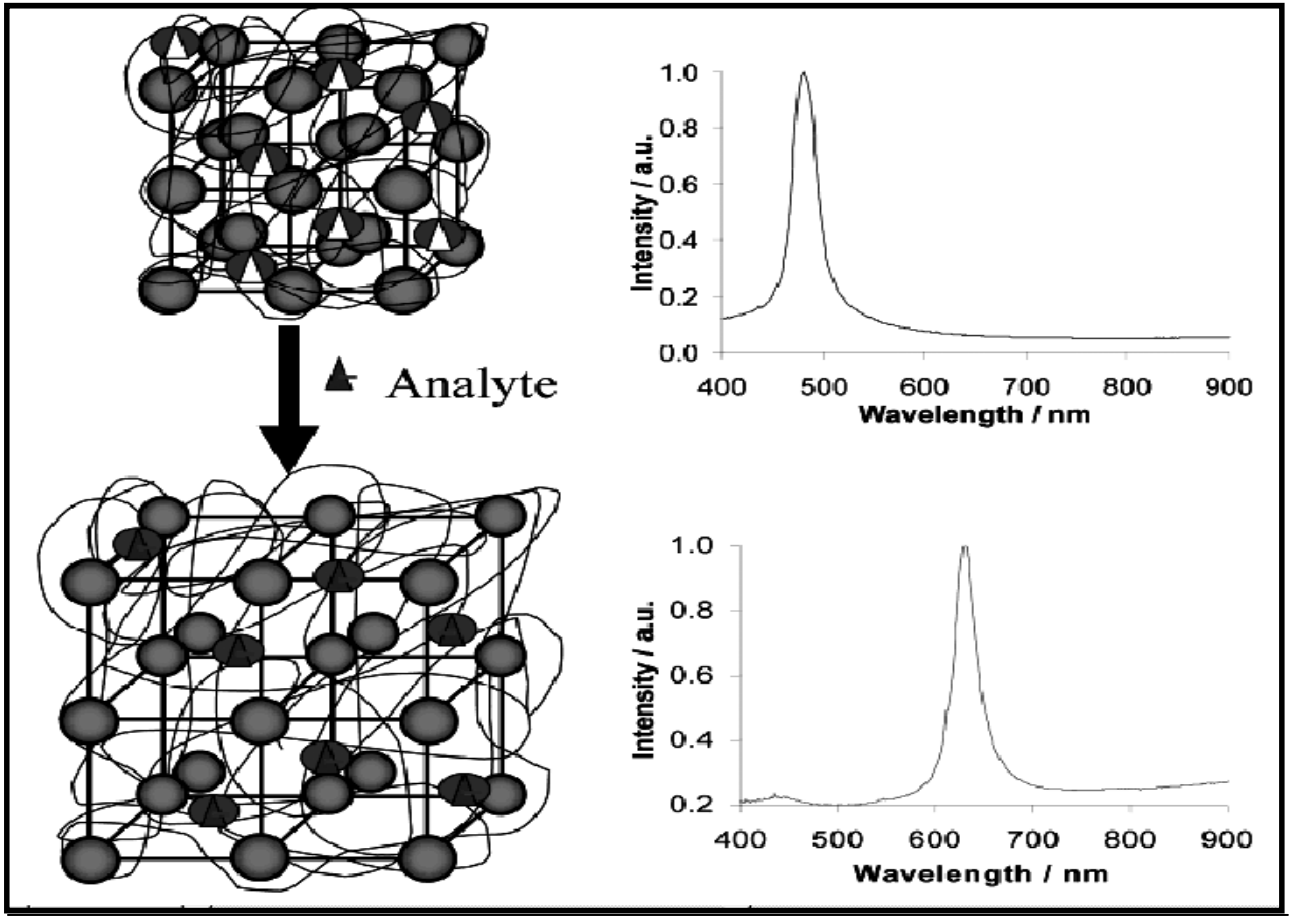

Figure 26.18 A sensor device developed on the basis of a colloidal array PBG embedded in a polymer hydrogel with molecular recognition elements. Upon swelling with analyte, the volume of the hydrogel expands, resulting in a spectral red shift (Reproduced with permission from American Chemical Society and authors; Reference 49).